On the Structural Role of the Aromatic Residue Environment of the Chlorophyll *a* in the Cytochrome b_6f Complex[†]

Jiusheng Yan,[‡,§] Naranbaatar Dashdorj,[||,⊥] Danas Baniulis,[‡,#] Eiki Yamashita,[‡,¶] Sergei Savikhin,[||] and William A. Cramer*[,‡]

Departments of Biological Sciences and Physics, Purdue University, West Lafayette, Indiana 47907

Received November 20, 2007; Revised Manuscript Received February 1, 2008

ABSTRACT: Because light is not required for catalytic turnover of the cytochrome b_6f complex, the role of the single chlorophyll *a* in the structure and function of the complex is enigmatic. Photodamage from this pigment is minimized by its short singlet excited-state lifetime (~200 ps), which has been attributed to quenching by nearby aromatic residues (Dashdorj et al., 2005). The crystal structure of the complex shows that the fifth ligand of the chlorophyll *a* contains two water molecules. On the basis of this structure, the properties of the bound chlorophyll and the complex were studied in the cyanobacterium, *Synechococcus* sp. PCC 7002, through site-directed mutagenesis of aromatic amino acids in the binding niche of the chlorophyll. The b_6f complex was purified from three mutant strains, a double mutant Phe133Leu/Phe135Leu in subunit IV and single mutants Tyr112Phe and Trp125Leu in the cytochrome b_6 subunit. The purified b_6f complex from Tyr112Phe or Phe133Leu/Phe135Leu mutants was characterized by (i) a loss of bound Chl and *b* heme, (ii) a shift in the absorbance peak and increase in bandwidth, (iii) multiple lifetime components, including one of 1.35 ns, and (iv) relatively small time-resolved absorbance anisotropy values of the Chl Q_y band. A change in these properties was minimal in the Trp125Leu mutant. *In vivo*, no decrease in electron-transport efficiency was detected in any of the mutants. It was concluded that (a) perturbation of its aromatic residue niche influences the stability of the Chl *a* and one or both *b* hemes in the monomer of the b_6f complex, and (b) Phe residues (Phe133/Phe135) of subunit IV are important in maintaining the short lifetime of the Chl *a* singlet excited state, thereby decreasing the probability of singlet oxygen formation.

The cytochrome b_6f complex functions in oxygenic photosynthetic membranes by catalyzing oxidation of plastoquinol and reduction of plastocyanin or cytochrome c_6. It thereby mediates electron transfer from photosystem (PS) II to PS I in the linear photosynthetic electron-transfer pathway from H_2O to $NADP^+$ and contributes to the electrochemical proton gradient generated across the membrane that is used for ATP synthesis (*1, 2*). Crystal structures of the b_6f complex from the thermophilic cyanobacterium *Mastigocladus laminosus* have been obtained to a resolution of 3.0 Å (*3*), in the presence of the quinone analogue inhibitor, DBMIB, to 3.8 Å (*4*), in the native state to a resolution of 3.0 Å (*5*), and in the presence of the quinone analogues tridecyl-stigmatellin (TDS) and NQNO to 3.40 Å and 3.55 Å (*5*). The complex was solved from the green alga, *Chlamydomonas reinhardtii*, in the presence of TDS to a resolution of 3.1 Å. The b_6f complex is a 220 kDa homodimeric complex composed of 8 subunits with 13 transmembrane helices in each monomer, 2 p-side extramembrane soluble domains, and 7 prosthetic groups per monomer: 4 hemes, 1 [2Fe−2S] cluster, 1 chlorophyll (Chl)[1] *a*, and 1 *β*-carotene (Figure 1A). The cytochrome b_6 subunit contains four transmembrane helices, two noncovalently bound hemes (b_p and b_n), located near the p- and n-sides of the membrane, and a novel n-side covalently bound heme, heme c_n (*2, 3, 6*). With subunit IV, it forms the core of each monomer, whose hydrophobic nature is conserved between the b_6f and bc_1 complexes (*7*).

Four small hydrophobic subunits (MW = 3.3–4.3 kDa), Pet-G, -L, -M and -N, each having a single transmembrane helix, enclose the cytochrome b_6/subunit IV core of each

[†] These studies were supported by Grants from the NIH GM-38323 (to W.A.C.) and NSF (MCB-0516939). The structure of the environment of the bound Chl *a* resulted from experiments carried out at beam line SBC-19ID at the Advanced Photon Source, Argonne National Laboratory, supported by DOE W31-109ENG389.

* To whom correspondence should be addressed. Telephone: (765) 494-4956. Fax: (765) 496-1189. E-mail: waclab@purdue.edu.

[‡] Department of Biological Sciences.

[§] Current address: Section of Neurobiology, School of Biological Sciences, University of Texas, Austin, TX 78713.

[||] Department of Physics.

[⊥] Current address: Laboratory of Chemical Physics, National Institute of Diabetes and Digestive and Kidney Diseases (NIDDK), National Institutes of Health (NIH), Bethesda, MD 20892.

[#] Current address: Lithuanian Institute of Horticulture, Babtai, Kaunas reg., LT 54333, Lithuania.

[¶] Current address: Institute for Protein Research, Osaka University, Osaka 565-0871, Japan.

[1] Abbreviations: Chl, chlorophyll; Cyt, cytochrome; DCMU, 3-(3′,4′-dichlorphenyl)-1,1-dimethylurea; FCCP, carbonyl cyanide *p*-trifluoromethoxy-phenylhydrazone; fwhm, full width at half-maximum; p- and n-, positive and negative sides of transmembrane electrochemical potential gradient, respectively; PCR, polymerase chain reaction; PDB, Protein Data Bank; SDS−PAGE, sodium dodecyl sulfate−polyacrylamide gel electrophoresis; WT^{HS} and WT^{HSK}, strains of *Synechococcus* sp. PCC 7002 that express the His_6-tagged b_6f complex that are resistant, to spectinomycin or spectinomycin and kanomycin.

10.1021/bi702299b CCC: $40.75
Published on Web 02/27/2008

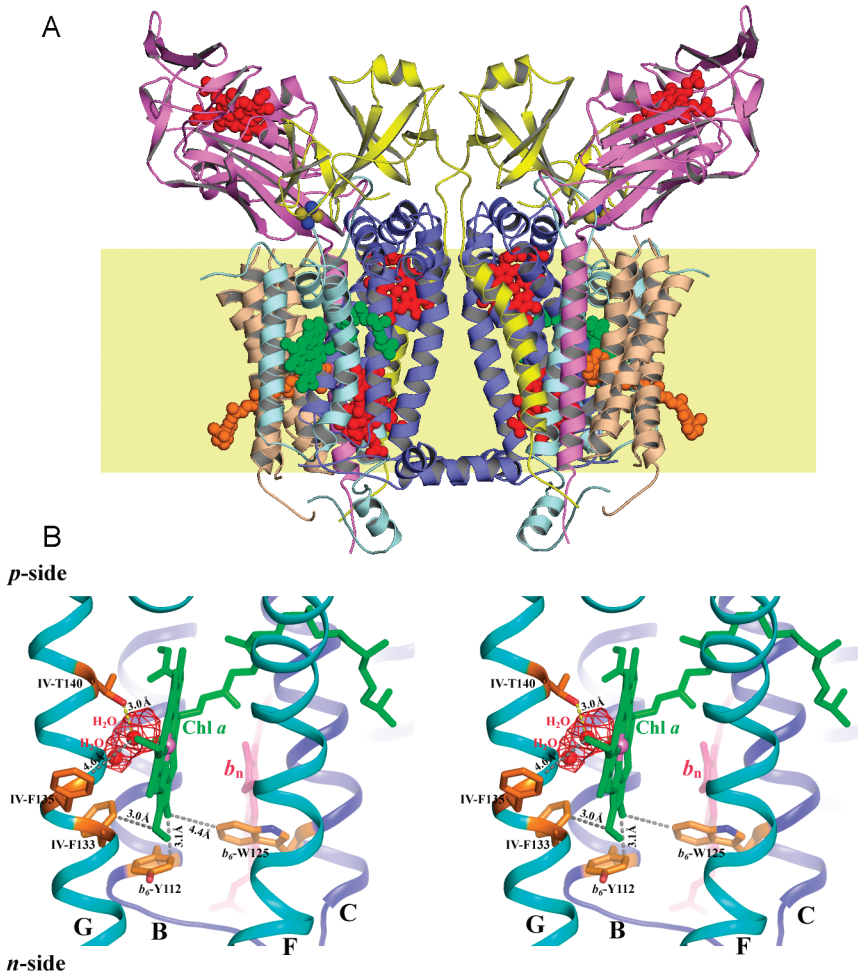

FIGURE 1: (A) Structure (view parallel to the membrane plane) of the cytochrome b_6f complex from the thermophilic cyanobacterium *M. laminosus* (PDB code 2E74). The overall dimensions of the dimer in this profile are 100 × 120 Å. Color code for different subunits: cytochrome b_6, blue; subunit IV, cyan; cytochrome *f*, violet; ISP, yellow; small subunits (petG, -L, -M, and -N), wheat. Prosthetic groups displayed in space-filling diagrams are chlorophyll (green), β-carotene (orange), all hemes (red), and ion (blue)−sulfur (yellow) cluster. The membrane bilayer is shown in shallow yellow. (B) Binding niche of the chlorophyll *a* porphyrin ring. Mutated residues are shown in sticks, and their distance to the porphyrin ring is indicated. Labels, B, C, F, and G refer to a transmembrane helix in cytochrome b_6 (B and C) or subunit IV (F and G). Coordination of chlorophyll Mg by two water molecules is shown.

monomer. The cytochrome *f* and ISP subunits individually form a large extra-membrane p-side soluble domain that contain, respectively, a *c*-type heme and [2Fe−2S] cluster and are embedded in the membrane by a single C- or N-terminal transmembrane helix. The core of the cytochrome b_6f complex is structurally analogous to that of the cytochrome bc_1 complex of the mitochondrial respiratory chain and photosynthetic bacteria (*8, 9*). The charge-transfer functions are generally thought to be similar, although the presence of heme c_n creates a significant difference in structure with consequences for function (*2, 5, 10*).

The b_6f complex also contains one Chl *a* and one carotenoid molecule per monomer. The porphyrin ring of the chlorophyll molecule is inserted between the F and G helices of subunit IV (Figure 1A), and its phytyl chain extends into a portal on the p-side of the intermonomer cavity (*3, 6, 11*). The function of the Chl *a* in the b_6f complex is enigmatic, because no light reaction is required for enzymatic turnover of the complex. The rate at which light is absorbed by the Chl *a* under normal daylight intensity is 5–10 photons s^{-1}, a factor of ~100, smaller than the rate of turnover (~5×10^2 s^{-1}) of the b_6f complex.

The unit pigment stoichiometry makes this a unique system for the study of intraprotein pigment–protein interactions without interference from other pigment molecules (*12*). A special feature of the single chlorophyll *a* in the complex is its short singlet excited-state lifetime ($\tau \sim 200$ ps), with a resultant low quantum yield of the excited triplet and yield of excited triplet state (*12, 13*). This provides at least part of the mechanism for protection of the chlorophyll from photodamage, resulting from the generation of singlet oxygen (*13*). Additional protection is achieved through an unusual long-range intraprotein chlorophyll−carotenoid triplet energy transfer (*14*). It was proposed that the short lifetime resulted from quenching of the chlorophyll singlet excited-state by one or more aromatic residues closest to the chlorophyll (*12, 13*). In the b_6f structure, the chlorophyll porphyrin ring is bound in a region enriched with aromatic residues (*3, 5, 6, 13*). The nearest prosthetic group to the chlorophyll ring is the n-side heme b_n, one of the two bis-histidine coordinated *b* hemes that spans the membrane, which is separated from the Chl *a* by 5.5 Å edge−edge (*3, 6*).

The present study concerns the interactions of the unique Chl *a* with the neighboring aromatic amino acids and the

consequences for the structure of the b_6f complex of alteration of these residues by mutagenesis.

MATERIALS AND METHODS

Growth of Cultures. Synechococcus sp. PCC 7002 cells were grown in medium A (*15*), supplemented with 100 μg mL^{-1} spectinomycin for strain WT^{HS} and 50 μg mL^{-1} kanomycin for strains WT^{HSK}, b_6-Y112F, b_6-W125L, and IV-F133L/F135L. Liquid cultures were grown at 38 °C under cool-white fluorescent illumination at a light intensity of ~100 μEinstein m^{-2} s^{-1}, bubbled with air supplemented with ~2% (v/v) CO_2.

Construction of Mutant Strains of Synechococcus sp. PCC 7002. To facilitate protein purification, a mutant strain, WT^{HS}, which expresses the His$_6$-tagged cytochrome *f* and is resistant to spectinomycin, was constructed. A plasmid pCA1-LH, which contains an exogenous *Eco*R I site and a His$_6$ tag at the 3′ terminus of *petA* and a 0.9 kb 3′ flanking sequence of *petA*, was constructed with the template plasmids of pCA2 and pCA1 (*16*), and the PCR product of *petA* 3′-side flanking sequence from the *Synechococcus* genome. The plasmid pCA1-LH was transformed to the *Synechococcus* sp. PCC 7002 wild-type strain as previously described (*16*). To screen for the complete segregant of the mutant strain WT^{HS}, a 1.1 kb DNA fragment containing the entire *petA* and a 0.1 kb 3′ flanking sequence was amplified from the genomic DNA of the transformants that survived on a medium A plate supplemented with 100 μg mL^{-1} spectinomycin. Complete segregation and absence of the wild-type allele in the *Synechococcus* genome were confirmed by complete digestion of the PCR product by *Eco*R I and also by sequencing of the PCR products.

A control strain, WT^{HSK}, and Chl *a* binding-niche mutant strains, b_6-Y112F, b_6-W125L, and IV-F133L/F135, which contain a His$_6$-tagged cytochrome *f* and wild-type cytochrome b_6 and subunit IV or the indicated mutations on cytochrome b_6 ("b_6") or subunit IV ("IV"), were constructed as described below. The corresponding mutations of *petB* or *petD* were performed by PCR-based site-directed mutagenesis (QuikChange, Stratagene) with plasmid pBD2 (*11*) that contains the *petBD* operon. The pBD2 plasmid bearing either the wild-type *petBD* for generation of control strain WT^{HSK} or mutated *petBD* was transformed to the WT^{HS} strain of *Synechococcus*. Complete segregants were selected on plates supplemented with kanomycin and screened for construction of cytochrome b_6 and subunit IV mutants, as previously described (*11*).

Purification of the His$_6$-Tagged Cytochrome b_6f Complex from Synechococcus sp. PCC 7002. Late log-phase *Synechococcus* in liquid culture (40 L) was collected and resuspended in 150 mL "grinding buffer" (25 mM HEPES at pH 7.5, 0.2 M sucrose, 0.1% lysozyme, 10 mM $CaCl_2$, and 10 mM $MgCl_2$), containing the protease inhibitors 2 mM benzamidine, 2 mM amino-caproic acid, and 0.25 mM PMSF ("protease cocktail"), and incubated at room temperature for 2 h. The cells were broken by passage (4 times) through a French press operated at 18 000 PSI. Thylakoid membranes were collected by centrifugation at 118000*g* (Beckman, Ti70 rotor, 30 min). Membrane sediments were resuspended in 150 mL of 20 mM Tris-HCl at pH 7.0, with the protease cocktail, collected by centrifugation at 118000*g* (25 min), and sediments were resuspended in 100 mL of TBS buffer (10 mM Tricine-NaOH at pH 8.0, 2 M NaBr, and 0.4 M sucrose) and stirred at 4 °C (20 min). After dilution with an equal volume of cold distilled water, the suspension was again subjected to centrifugation at 118000*g* (20 min). The sediments were suspended in 150 mL of 20 mM Tris-HCl at pH 7.0, with protease inhibitors, centrifuged, resuspended in a total volume of 60 mL in 20 mM Tris-HCl at pH 8.0 and 100 mM NaCl, with the protease cocktail, and then mixed with the same 60 mL buffer solution supplemented with 50 mM Hecameg (Anatrace, Maumee, OH) detergent (*17*). The suspension was incubated and stirred at 4 °C for 25 min and then centrifuged at 231000*g* for 45 min. The supernatant, which contains the extracted b_6f complex from the membranes, was loaded onto a nickel column (~4 mL of packed Ni−NTA resin) pre-equilibrated with "wash buffer" (20 mM Tris-HCl at pH 8.0, 10% glycerol, 0.1 M NaCl, 0.025% DDM, and 15 μg/ml DOPC, supplemented with protease inhibitors) at a flow rate of ~0.5 mL/min. The column was washed with ~200 mL of wash buffer until the eluant was free of absorbance from contaminating pigments (chlorophyll and carotenoids). The b_6f complex was eluted from the column with 10 mL of wash buffer supplemented with 50 mM histidine instead of imidazole to avoid denaturation of c-type cytochrome as occurred in isolation of the His-tagged cytochrome bc_1 complex (*18*). The eluted b_6f complex was pooled, concentrated with a Centricon, and stored at −70 °C.

Growth Rate Measurement and Oxygen Evolution. Cells were cultivated in 1.5 cm diameter tubes containing 20 mL of medium A supplemented with 50 μg mL^{-1} kanamycin and 2% CO_2 at 38 °C, under 200–250 μEinstein m^{-2} s^{-1} continuous illumination. The cell density was determined from the optical density at 730 nm. The oxygen evolution rate was measured using a Clark-type oxygen electrode at 38 °C, under 2.0–2.5 mEinstein m^{-2} s^{-1} illumination as described (*18*). Cells were suspended at 10 μg mL^{-1} Chl *a* in 5 mM HEPES-NaOH at pH 7.5, 10 mM NaCl, and 10 mM $NaHCO_3$.

Spectroscopy. Optical chemical difference spectra were measured using a Cary 4000 UV–Vis spectrophotometer using a full width at half-maximum (fwhm) of 1 nm, so that the measured spectral peaks and bandwidths were accurate to ±0.2 nm. Chemical difference spectra that defined cytochrome content were obtained as described previously (*19, 20*) with ascorbate and dithionite as reductants and ferricyanide as the oxidant. Ultrafast transient absorption differences (ΔA) and time-resolved chlorophyll absorbance anisotropy following optical excitation were measured using the femtosecond pump–probe spectrometer described in ref *13*. The latter setup enabled the measurement of kinetic lifetimes in the range of 0.4–700 ps to within ~10% precision. For the lifetimes longer than 700 ps (time span of the measurement window), the precision becomes progressively smaller with the upper error margin being substantially larger than the lower error margin. Both upper and lower error margins are shown (Table 1).

Flash Kinetic Spectroscopy. Flash-induced oxidation and re-reduction of cytochrome f/c_6 in intact cells of *Synechococcus* sp. PCC 7002, resuspended at 5 μM chlorophyll in 50 mM HEPES at pH 7.5, 0.1 M NaCl, 10 mM $NaHCO_3$, 10 μM DCMU, 10 μM FCCP, and 1 mM KCN, was monitored in the α-band absorbance region ($\Delta A_{556–540}$), using

Table 1: Optical Properties and Content of Chl *a* and *b* Heme in the b_6f Complex from *Synechococcus* and Crystals from *M. laminosus*

	properties of Chl *a* specifically bound to b_6f					properties of *b* hemes	
cyanobacterium	stoichiometry	Q_y band maxima (nm)	Q_y band fwhm (nm)	singlet excited-state lifetime(s)	time-resolved anisotropy ($t = 0$)	stoichiometry (*b*/*f*)	absorbance maximum (nm)
Synechococcus WT^{HS}	1.0 ± 0.05 ($n = 3$)[a]	672 ± 0.2 nm ($n = 3$)	17 ± 0.5 nm ($n = 3$)	203 ± 20 ps	0.37 ± 0.01	2.0 ± 0.05 ($n = 3$)	564.0
Synechococcus b_6-W125L[b]	0.8	672 nm	17 nm	200 ± 20 ps	0.37 ± 0.01	1.8	564.0
Synechococcus b_6-Y112F	0.81 ± 0.36 ($n = 3$)	674.5 ± 0.6 nm ($n = 3$)	20.6 ± 0.7 nm ($n = 3$)	188 ± 20 ps	0.11 ± 0.01	1.42 ± 0.06 ($n = 3$)	564.0
Synechococcus IV-F133L/F135L	0.72 ± 0.2 ($n = 4$)	674 ± 1.0 nm ($n = 4$)	27.6 ± 1.2 nm ($n = 4$)	0.43, 4.1, 27.3 ps; $1.35 + 2$ or -0.4 ns[c]	0.13 ± 0.01	1.04 ± 0.18 ($n = 6$)	564.0
M. laminosus, crystal	1.0	671.5 nm	17 ± 0.5 nm	200 ± 20 ps	0.37 ± 0.01	2.0	564.0

[a] n = number of different preparations assayed. [b] $n = 1$. [c] The Chl *a* pocket in this mutant can have multiple conformations, each characterized by a different lifetime, as shown by the respective DAS (Figure 3C) and discussed in Figure 3C and the Discussion.

a laboratory-built single-beam spectrometer with an Xe flash actinic source, as previously described (*16, 19*).

Crystallization, Crystallography, and Crystallographic Analysis. The coordinates of the native b_6f complex that contain the description of the environment of the bound chlorophyll *a* are contained in the PDB (code 2E74). The details of the structure analysis and the data refinement for the native crystal and two complexes with two different quinone analogue inhibitors are provided (*5*), although no description of the detailed environment of the chlorophyll was provided in ref *5*.

RESULTS

Perturbation of the Chl a Binding Niche by Site-Directed Mutations. In the crystal structures of the b_6f complex, the porphyrin ring of the Chl *a* molecule is wedged between the F and G transmembrane helices of subunit IV in a region enriched with aromatic residues on both helices. The coordinates of the 3.0 Å crystal structure of the native b_6f complex revealed two connected waters as the axial fifth ligand of the Chl *a*, with the first water within hydrogen-bond distance of the hydroxyl of the Thr140 in subunit IV (*5*). Four aromatic residues are in close proximity (within 5 Å) of the Chl *a* porphyrin ring. The side chains of Tyr112 and Trp125 (residues 105 and 118 in *M. laminosus*) from the cytochrome b_6 subunit and Phe133 and Phe135 from subunit IV in the cyanobacterium *Synechococcus* sp. PCC 7002 are, respectively, 3.1, 4.4, 3.0, and 4.6 Å (edge−edge) from the porphyrin ring (Figure 1B) according to the structure of the *M. laminosus* b_6f complex (*3, 5*). These aromatic residues are conserved in cyanobacteria, algae, and higher plants. To perturb the binding environment of the porphyrin ring, point mutants of the corresponding residues were constructed by site-directed mutagenesis in *Synechococcus* sp. PCC 7002, in which the core subunits, cyt b_6 and subunit IV, are 86 and 73% identical compared to *M. laminosus*, and which is genetically transformable. Complete segregants were obtained for the single-substitution mutants, b_6-Y112F and b_6-W125L, and the double-substitution mutant, IV-F133L/F135L. It was not possible by extensive screening to isolate a segregant of the mutant b_6-Y112L, indicating that this mutation is lethal to the growth of the *Synechococcus* cells.

Purification of the His-Tagged Cytochrome b_6f Complex from Synechococcus sp. PCC 7002. Cyanobacteria have been used as a model system for structural and functional characterization of the cyt b_6f complex *in vivo* and *in vitro* (*1, 3, 21–25*). An active, dimeric cyanobacterial b_6f complex has previously been isolated and characterized from the thermophilic filamentous cyanobacterium, *M. laminosus* (*26*), which is nontransformable. Cytochrome b_6f complexes isolated from the two other cyanobacteria, *Synechocystis* sp. PCC 6803 and *Synechocystis* sp. PCC 6714, were shown to be inactive because of monomerization and/or loss of the Rieske iron−sulfur protein (*27, 28*). A similar result has been obtained with the thermophilic cyanobacterium, *Thermosynechococcus elongatus* (H. Zhang and W. A. Cramer, unpublished data). Using a His_6 tag at the C terminus of cytochrome *f*, the b_6f complex of the transformable cyanobacterium, *Synechococcus* sp. PCC 7002, was purified using a nickel-affinity column. Analysis of the isolated

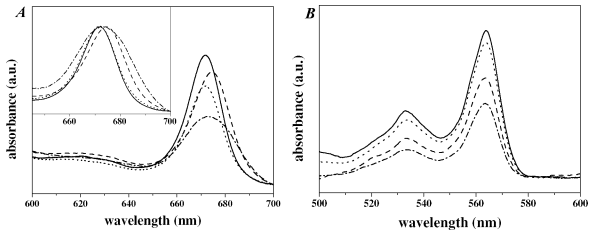

FIGURE 2: Representative absorbance spectra of the purified His-tagged b_6f complex from the control strain WT^{HS} (—) and Chl mutants, b_6-Y112F (- - -), b_6-W125L (• • •), and IV-F133L/F135L (- • -). (A) Absorption spectra of the chlorophyll *a* normalized to the same cytochrome *f* content to show decreased Chl content or normalized to the same peak height (inset) to show altered optical properties in Chl domain mutants. (B) Cytochrome difference spectra (dithionite reduced minus ascorbate reduced) of the b_6f complexes.

complex by sucrose-gradient centrifugation and EPR spectroscopy of the [2Fe−2S] cluster indicated that the isolated complex in the wild type is significantly (≥50%) monomerized and the integrity of the [2Fe−2S] iron−sulfur cluster mostly (≥90%) lost. However, as judged from absorbance spectra and SDS−PAGE of the whole complex and heme strain of the covalently bound heme c_n on SDS−PAGE gels (data not shown), the cyt b_6, subunit IV, and cyt *f* subunits including their prosthetic groups, hemes b_p, b_n, *f*, and c_n, Chl *a*, and β-carotene, remain intact in the isolated b_6f complex from the Chl *a* wild-type strains, WT^{HS} or WT^{HSK}.

Absorbance Spectra of Purified Cytochrome b_6f Complexes from Chl aMutant Strains. In contrast to the b_6f complex from wild-type strain, the isolated b_6f complex from the b_6-Y112F and IV-F133L/F135L strains showed a 20–50% decrease in amplitude of the Chl *a* Q_y visible absorbance band (Figure 2A and Table 1). Methanol extraction of Chl *a* in the isolated complex showed that the decreased peak intensity arose from a decrease in Chl *a* content and not from changes in the extinction coefficient. The absorbance spectrum of Chl *a* in mutant b_6-W125L is similar to that of the wild type in peak position and half-bandwidth. However, in comparison to the spectrum of the wild type, the Chl *a* Q_y band in the b_6-Y112F and IV-F133L/F135L mutants is red-shifted by 2.5 ± 0.6 and 2.0 ± 1.0 nm and is broadened by an increase in the half-bandwidth of 3.6 ± 0.7 and 10.6 ± 1.2 nm to 20.6 and 27.6 nm, respectively (Figure 2A and Table 1).

Chemical difference spectra (dithionite reduced minus ascorbate reduced) of the isolated complex showed that 29 ± 3 and 48 ± 9% of the *b* heme was lost, respectively, in the b_6-Y112F and IV-F133L/F135L mutants (Figure 2B and Table 1). The absorbance maximum of the residual *b* heme is the same, 564 ± 0.2 nm, in all mutants and the wild type. The lower content of *b* heme in these mutants was also confirmed by spectral measurement of the pyridine hemochromagen derivatives (data not shown). The loss of *b* heme was not caused by the presence of histidine in the nickel-column elution buffer during the purification process because elution of the His_6-tagged b_6f complex by EDTA or acid gave the same result. As judged from SDS−PAGE and heme strain of the covalently bound heme c_n, the loss of *b* heme does not result from the loss of the intact cytochrome b_6 polypeptide subunit from the membranes or isolated b_6f complex (data not shown). A proper ratio of cytochrome b_6 subunit and cytochrome *f* in these three mutants is also supported by the observation that, *in vivo*, (i) cytochrome *f* was fully re-reduced by a light flash at a rate similar to that of the wild type and most of the mutants and (ii) growth rates and O_2 evolution rates were the same in mutants and the wild type (Table 2). Because the *b* heme is required for the catalytic turnover of the b_6f complex, it is inferred that the complement of *b* heme remains intact *in vivo* but a significant fraction of the *b* heme was lost during purification.

Kinetics of the Chl a Singlet Excited State in Purified Cytochrome b_6f Complexes. The kinetics of the singlet excited state of the Chl *a* in the wild type and mutant b_6f complexes were probed by femtosecond time-resolved pump–probe spectroscopy. The samples were excited at 660 or 630 nm, and absorbance difference (ΔA) kinetics were recorded at a series of probe wavelengths covering the entire Q_y absorption band of Chl *a*. The time-resolved ΔA profiles at all probe wavelengths were globally fit with several decay components, and the probe wavelength-dependent amplitudes of these components were assembled into the decay-associated spectra (DAS) (Figure 3). Time-resolved ΔA profiles of His_6-tagged wild-type *Synechococcus* b_6f could be best-fit with a major decay component having a lifetime of 203 ± 20 ps (Figure 3A and Table 2), a decay profile that closely resembles the DAS of the ultrapure b_6f complex obtained with diffraction-quality crystals from *M. laminosus* (*13*). According to the latter study, the ~200 ps component corresponds to Chl *a* ground-state recovery kinetics. The analysis of ΔA profiles of the b_6-Y112F mutant yielded similar DAS components (Figure 3B), as did that of the b_6-W125L mutant (data not shown). In contrast, the ~200 ps component was absent in the IV-F133L/F135L mutant complex. Four decay components were required to fit the time-resolved absorbance spectra (Figure 3C), indicating that the binding of Chl *a* in this mutant is significantly perturbed and multiple binding modes are present. The 1.35 ns decay component, which is of significant amplitude for the IV-F133L/F135L mutant, has a spectral position similar to the ~200 ps component in the wild type and is tentatively attributed to the ground-state recovery kinetics of the specifically bound Chl *a*.

Time-Resolved Anisotropy of the Chl a in the Purified Cytochrome b_6f Complex. The anisotropy of the ΔA signal from the WT^{HS} complex (Figure 4A) and the b_6-W125L mutant were determined to be 0.37 ± 0.01. This value is identical to that obtained from dissolved crystals of the *M. laminosus* b_6f complex (*13*), and close to the theoretical maximum of 0.4 for a completely rigid molecule with parallel absorption and emission transition dipole moments. The anisotropy was found to be almost constant during the lifetime of the Chl *a* excited state, indicating that Chl *a* excitation does not lead to detectable reorientation of the molecule. In contrast, the b_6-Y112F and IV-F133L/F135L mutant complexes (parts B and C of Figure 4) exhibited a much lower anisotropy (0.11–0.13). The origin of these low anisotropy values observed on a very short time scale is discussed below (see the Discussion).

Electron-Transfer Activity of the Cytochrome b_6f Mutant Complexes. The rate-limiting electron-transfer step associated with the b_6f complex was measured in intact cells of *Synechococcus* sp. PCC 7002 through rates of reduction of cytochromes *f* and c_6, which have overlapping α-band

Table 2: Growth and Electron-Transport Parameters of *Synechococcus* sp. PCC 7002 Mutants

Synechococcus strain	doubling time (h)	oxygen evolution [μmol of O_2 (mg of Chl *a*)$^{-1}$ h^{-1}]	half-time for cytochrome f/c_6 reduction (ms)
Synechococcus WT^{HS}	6.1 ± 0.1	298 ± 12	10.6 ± 0.7
Synechococcus b_6-W125L	nd[a]	nd	2.6 ± 0.3
Synechococcus b_6-Y112F	6.3 ± 0.1	277 ± 10	8.9 ± 0.5
Synechococcus IV-F133L/F135L	6.6 ± 0.3	280 ± 6	11.6 ± 1.0

[a] nd = not determined.

spectra, after exposure to a light flash (*16*), as well as comparative rates of growth in culture and oxygen evolution (Table 2). A short saturating actinic flash triggered oxidation of PS I and a subsequent rapid oxidation ($t_1/_2$ = 100–200 μs) of cytochromes c_6 and *f*, which was followed by a relatively slow reduction ($t_1/_2$ = 10.6 ± 0.7 ms) of cytochromes *f* and c_6 in the control wild-type strain, WT^{HSK} (Table 1). The electron-transfer activity of the b_6f complex *in vivo* was not significantly affected by perturbations in the chlorophyll *a* binding niche in mutants, b_6-Y112F ($t_1/_2$ = 8.9 ± 0.5 ms for the reduction of cytochrome *f* and c_6) and IV-F133L/F135L ($t_1/_2$ = 11.6 ± 1.0 ms) (Table 2). In mutant b_6-W125L, the half-time ($t_1/_2$) for the reduction of cytochrome f/c_6 was 2.6 ± 0.3 ms. This increase of electron-transfer activity in the mutant b_6-W125L may be caused by a direct effect of heme b_n, because the mutation site (b_6-W125) is only 4.0 Å (edge−edge) to the heme. The observation of an altered electron-transfer rate in the high-potential chain (p side) by mutations around the Q_n site has been reported (*25, 29*).

DISCUSSION

Quenching Mechanism of the Chl a Singlet Excited State. The singlet excited-state lifetime of the Chl *a* in the isolated cytochrome b_6f complex is ~200 ps (*12, 13*), which is ~25 times shorter than the 5–6 ns lifetime reported for monomeric Chl *a* molecules in solution (*30*). It was proposed that the quenching of the Chl *a* singlet excited state was due to the excitation-induced electron exchange between the Chl *a* and nearby aromatic amino acid residue(s) (*12*), particularly the Tyr and Trp residues that can function as an electron acceptor/donor in a charge-exchange mechanism of fluorescence quenching (*13*). Four highly conserved aromatic residues, Tyr112 and Trp125 of cytochrome b_6 and Phe133 and Phe135 of subunit IV, are within 5 Å of the Chl *a* porphyrin ring in the *Synechococcus* b_6f complex (Figure 1B). The kinetics of the Chl *a* singlet excited state in b_6-Y112F and b_6-W125L mutant complexes turned out to be similar to those measured for the wild-type b_6f complex, implying that neither Tyr112 nor Trp125 of the cytochrome b_6 subunit is responsible for quenching the Chl *a* singlet excited state, contrary to our earlier inference (*13*). However, the dominant ~200 ps component was replaced by a much slower component (1.35 ns) in the ultrafast singlet excited-state kinetics of the Chl *a* in the IV-F133L/F135L mutant (Table 1). The Phe residues could, in principle, be responsible for the quenching mediated by electron transfer if they have suitable redox potentials. However, these are currently unknown, and Phe is reportedly a less efficient donor than Tyr or Trp (*31, 32*).

Mutations Affecting the Aromatic Residue Environment around Chl a. Aromatic residues may have a role in stabilizing the configuration of the porphyrin ring through $\pi-\pi$ electronic interactions in the b_6f complex (*13*). Except for a ~20% loss of the Chl *a* content, the mutation b_6-W125L has little effect on the optical properties of the Chl *a*. Removal of the hydroxy group of Tyr112 by substitution with Phe (mutation b_6-Y112F) caused a 2–3 nm red shift, a 4–5 nm broadening of the Q_y absorption band, and a substantially decreased time-resolved anisotropy (Table 1). A more significant change in the Chl *a* binding and optical properties was shown in the double-substitution mutant, IV-F133L/F135L. These altered spectroscopic properties of the Chl *a* Q_y band in the b_6-Y112F and IV-F133L/F135L mutants, together with the decreased stoichiometry of bound Chl, can be attributed to more weakly bound Chl *a*.

Low Anisotropy Values. It is unlikely that the lower anisotropy levels observed in b_6-Y112F and IV-F133L/F135L can be attributed to increased rotational mobility of the Chl *a*, because that would require significant motion of the relatively large Chl molecule on a pico- or sub-picosecond time scale. Alternatively, the low initial anisotropy level of the b_6-Y112F mutant can be explained by a change in the orientation/polarization of the excited-state transition moment (*33*). A different explanation is proposed for the low initial anisotropy of the IV-F133L/F135L. Together with the multiple lifetime components, it is most readily explained by the assumption that these features stem from aggregated (excitonic) forms of nonspecifically bound Chl, which would also be consistent with the ~10 nm spectral shift of the respective DAS (Figure 3C). The initial ~30 ps rise in the anisotropy in the case of IV-F133L/F135L (Figure 4C) is

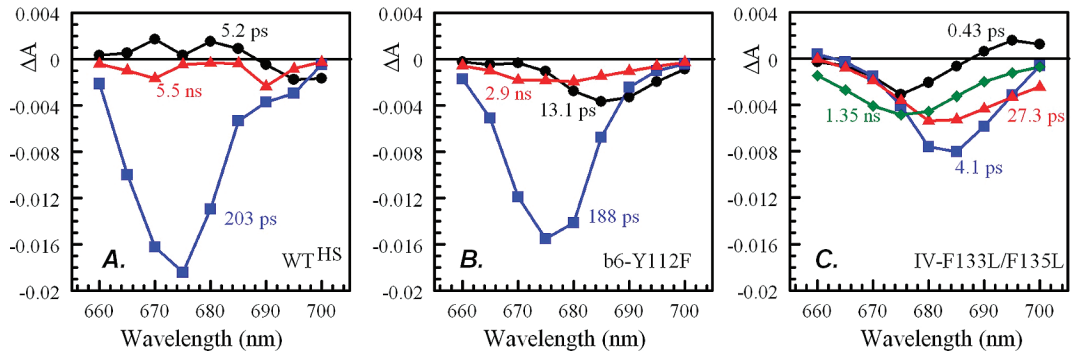

FIGURE 3: Decay-associated spectra obtained by global analysis of transient time-resolved absorption difference (ΔA) profiles for the Chl *a* in the isolated b_6f complex from control strain WT^{HS} (A) and Chl *a* mutant strains, b_6-Y112F (B) and IV-F133L/F135L (C). Lifetimes were determined to within ~10% precision, except the 1.35 ns, for which precision is +2 or −0.4 ns.

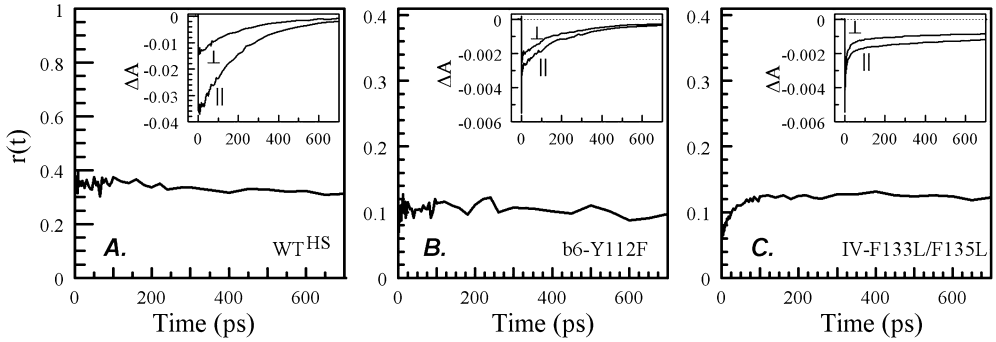

FIGURE 4: Time-resolved anisotropy $r(t)$ of ΔA signal probed at 680 nm for the WT^{HS} (A), b_6-Y112F (B) and IV-F133L/F135L (C) b_6f complexes. (Inset) Corresponding anisotropic $\Delta A_{||}$ and $\Delta A_{\perp}$ profiles.

readily reproduced in a model where the ΔA signals responsible for the 4.1 ± 0.4 and 27 ± 3 ps components in the DAS (Figure 3C) are fully depolarized at all times and the 1.35 ns component has a constant anisotropy similar to the anisotropy of the 188 ± 20 ps component in the b_6-Y112F mutant. In summary, the changes in Chl *a* lifetime and anisotropy imply that both the b_6-Y112F and IV-F133L/F135L mutations lead to significant perturbation of the binding niche of Chl *a*.

Structure of the Chl a Binding Niche. In structures of other Chl proteins, Chl *a* molecules have an axial fifth ligand that is either an amino acid side chain or one H_2O. In the 3.0 Å native b_6f structure (*7*), the Chl central Mg is coordinated by a pair of hydrogen-bonded water molecules, one ligated to the Mg atoms and the other hydrogen-bonded to the peptide side chain and backbone of the G helix of subunit IV. This side of the Chl phorphyrin ring, where the $C13^2$-(*R*)-methoxycarbonyl moiety protrudes, is energetically favorable for ligand binding (*34*). Although the coordination state of the Chl may slightly affect its fluorescence lifetime (*35*), there is no evidence for a large ligand-induced decrease of the fluorescence or singlet excited-state lifetime. According to the 3.0 Å native structure of the *M. laminosus* b_6f complex (*5*), the Trp79 and Tyr80 of subunit IV, which is part of the important PEWY motif (*7, 36*), are also not far from the Chl, ~8.5 Å from the Trp/Tyr aromatic ring to Chl ring and 5–6 Å to the Chl $C13^2$-(*R*)-methoxycarbonyl group. Whereas the two residues, Phe133/Phe135, are necessary for proper binding of the Chl and their mutation results in an increased lifetime (Table 1), one or both of Trp79/Tyr80 could also contribute to the decrease in lifetime of the Chl singlet excited state from 5 to 6 ns to 200 ps (*12, 13*).

Functions of Chl a. Three functions have been proposed for the Chl *a* molecule in the b_6f complex (*37*): (i) Facilitation of electron transfer. The loss of the Chl *a* in the b_6f complex isolated from the mutants arises from either a low occupancy *in vivo* or the loss of Chl *a* during purification of the complex. In either case, the binding of Chl *a* in these mutants is weakened. However, the electron-transfer activity, measured by the rate-limiting time course of cytochrome *f* reduction in intact cells, is not significantly changed in these mutants (Table 2). This indicates that perturbation of the Chl *a* does not inhibit the electron-transfer function of the b_6f complex *in vivo*. This is consistent with the absence *in vitro* of an inhibition of electron-transfer activity by photobleaching of Chl *a* (*37*). It is not known whether any pigment or heme is lost in the mutants *in vivo*. (ii) Regulation of b_6f assembly. It has been reported that accumulation of b_6f was not observed in the *Chlamydomonas reinhardtii* mutant ΔGid, which does not synthesize any Chl (*37*). (iii) The unique chlorophyll stabilizes the structure. The role of the Chl *a* in the b_6f complex might be considered in the perspective of Chl acting as a special lipid molecule that is an internal strut stabilizing the complex (*3*). There is a major loss (20–50%) of *b* heme in the b_6f complex isolated from the b_6-Y112F and IV-F133L/F135L mutants, although the amount of cytochrome b_6 polypeptide subunit was not decreased. Because the *b* heme is required for the electron transport through the b_6f complex and the electron-transfer activity of these three mutants *in vivo* was similar to that of control strain WT^{HSK}, it is concluded that *b* heme was lost during purification. The removal of *b* heme appears to be correlated with the altered binding or loss of Chl *a* (Table 1), which may result in the destabilization of local or global structure and consequently a loss of *b* heme during protein purification. The distance between the Chl *a* and heme b_n is only 5.5 Å in the *M. laminosus* structure (*3, 5*), and a direct interaction between heme b_n and Chl *a* could be inferrred from a small (1 nm) spectral shift of Chl *a* (at low temperature) as *b* heme was reduced in the b_6f complex of *Synechocystis* sp. PCC 6803 (*24*). Thus, Chl *a* may be involved in the stabilization of the structure of the b_6f complex and the *b* heme in particular.

SUPPORTING INFORMATION AVAILABLE

Original absorption difference profiles probed at nine wavelengths ranging from 660 to 700 nm for WT^{HS} (Figure S1), b_6-Y112F (Figure S2), and IV-F133L/F135L (Figure S3) samples; for each sample, the data fit globally with three to four decay components common to all nine profiles and varying amplitudes; amplitudes for these components then assembled into decay-associated spectra (DAS), as shown in Figure 3; and the original experimental profiles overlapped with the fits to the data (smooth curves). This material is available free of charge via the Internet at http://pubs.acs.org.

REFERENCES

1. Kallas, T. (1994) The cytochrome b_6f complex, in *The Molecular Biology of Cyanobacteria* (Bryant, D. A., Ed.) pp 259–317, Kluwer Academic Publishers Group, Dordrecht, The Netherlands.
2. Cramer, W. A., Zhang, H., Yan, J., Kurisu, G., and Smith, J. L. (2006) Transmembrane traffic in the cytochrome b_6f complex. *Annu. Rev. Biochem. 75*, 769–790.
3. Kurisu, G., Zhang, H., Smith, J. L., and Cramer, W. A. (2003) Structure of the cytochrome b_6f complex of oxygenic photosynthesis: Tuning the cavity. *Science 302*, 1009–1014.

4. Yan, J., Kurisu, G., and Cramer, W. A. (2006) Intraprotein transfer of the quinone analogue inhibitor 2,5-dibromo-3-methyl-6-isopropyl-*p*-benzoquinone in the cytochrome b_6f complex. *Proc. Natl. Acad. Sci. U.S.A. 103*, 69–74.
5. Yamashita, E., Zhang, H., and Cramer, W. A. (2007) Structure of the cytochrome b_6f complex: Quinone analogue inhibitors as ligands of heme c_n. *J. Mol. Biol. 370*, 39–52.
6. Stroebel, D., Choquet, Y., Popot, J. L., and Picot, D. (2003) An atypical haem in the cytochrome b_6f complex. *Nature 426*, 413–418.
7. Widger, W. R., Cramer, W. A., Herrmann, R. G., and Trebst, A. (1984) Sequence homology and structural similarity between cytochrome *b* of mitochondrial complex III and the chloroplast b_6f complex: Position of the cytochrome *b* hemes in the membrane. *Proc. Natl. Acad. Sci. U.S.A. 81*, 674–678.
8. Berry, E. A., Guergova-Kuras, M., Huang, L. S., and Crofts, A. R. (2000) Structure and function of cytochrome *bc* complexes. *Annu. Rev. Biochem. 69*, 1005–1075.
9. Smith, J. L., Zhang, H., Yan, J., Kurisu, G., and Cramer, W. A. (2004) Cytochrome *bc* complexes: A common core of structure and function surrounded by diversity in the outlying provinces. *Curr. Opin. Struct. Biol. 14*, 432–439.
10. Zatsman, A. I., Zhang, H., Gunderson, W. A., Cramer, W. A., and Hendrich, M. (2006) Heme–heme interactions in the cytochrome b_6f complex: EPR spectroscopy and correlation with structure. *J. Am. Chem. Soc. 128*, 14246–14247.
11. Yan, J., and Cramer, W. A. (2004) Molecular control of a bimodal distribution of quinone-analogue inhibitor binding sites in the cytochrome b_6f complex. *J. Mol. Biol. 344*, 481–493.
12. Peterman, E. J., Wenk, S. O., Pullerits, T., Palsson, L. O., van Grondelle, R., Dekker, J. P., Rogner, M., and van Amerongen, H. (1998) Fluorescence and absorption spectroscopy of the weakly fluorescent chlorophyll *a* in cytochrome b_6f of *Synechocystis* PCC 6803. *Biophys. J. 75*, 389–398.
13. Dashdorj, N., Zhang, H., Kim, H., Yan, J., Cramer, W. A., and Savikhin, S. (2005) The single chlorophyll *a* molecule in the cytochrome b_6f complex: Unusual optical properties protect the complex against singlet oxygen. *Biophys. J. 88*, 4178–4187.
14. Kim, H., Dashdorj, N., Zhang, H., Yan, J., Cramer, W. A., and Savikhin, S. (2005) An anomalous distance dependence of intraprotein chlorophyll-carotenoid triplet energy transfer. *Biophys. J. 89*, L28–L30.
15. Buzby, J. S., Porter, R. D., and Stevens, S. E., Jr. (1985) Expression of the *Escherichia coli lacZ* gene on a plasmid vector in a cyanobacterium. *Science 230*, 805–807.
16. Yan, J., and Cramer, W. A. (2003) Functional insensitivity of the cytochrome b_6f complex to structure changes in the hinge region of the Rieske iron−sulfur protein. *J. Biol. Chem. 278*, 20925–20933.
17. Pierre, Y., Breyton, C., Kramer, D., and Popot, J. L. (1995) Purification and characterization of the cytochrome b_6f complex from *Chlamydomonas reinhardtii*. *J. Biol. Chem. 270*, 29342–29349.
18. Guergova-Kuras, M., Salcedo-Hernandez, R., Bechmann, G., Kuras, R., Gennis, R. B., and Crofts, A. R. (1999) Expression and one-step purification of a fully active polyhistidine-tagged cytochrome bc_1 complex from *Rhodobacter sphaeroides*. *Protein Expression Purif. 15*, 370–380.
19. Ponamarev, M. V., and Cramer, W. A. (1998) Perturbation of the internal water chain in cytochrome *f* of oxygenic photosynthesis: Loss of the concerted reduction of cytochromes *f* and b_6. *Biochemistry 37*, 17199–17208.
20. Zhang, H., Huang, D., and Cramer, W. A. (1999) Stoichiometrically bound β-carotene in the cytochrome b_6f complex of oxygenic photosynthesis protects against oxygen damage. *J. Biol. Chem. 274*, 1581–1587.
21. Volkmer, T., Schneider, D., Bernat, G., Kirchhoff, H., Wenk, S. O., and Rogner, M. (2007) Ssr2998 of *Synechocystis* sp. PCC 6803 is involved in regulation of cyanobacterial electron transport and associated with the cytochrome b_6f complex. *J. Biol. Chem. 282*, 3730–3737.
22. Schneider, D., Berry, S., Rich, P., Seidler, A., and Rogner, M. (2001) A regulatory role of the PetM subunit in a cyanobacterial cytochrome b_6f complex. *J. Biol. Chem. 276*, 16780–16785.
23. Rogner, M., Nixon, P. J., and Diner, B. A. (1990) Purification and characterization of photosystem I and photosystem II core complexes from wild-type and phycocyanin-deficient strains of the cyanobacterium *Synechocystis* PCC 6803. *J. Biol. Chem. 265*, 6189–6196.
24. Wenk, S. O., Schneider, D., Boronowsky, U., Jager, C., Klughammer, C., de Weerd, F. L., van Roon, H., Vermaas, W. F., Dekker, J. P., and Rogner, M. (2005) Functional implications of pigments bound to a cyanobacterial cytochrome b_6f complex. *FEBS J. 272*, 582–592.
25. Nelson, M. E., Finazzi, G., Wang, Q. J., Middleton-Zarka, K. A., Whitmarsh, J., and Kallas, T. (2005) Cytochrome b_6 arginine 214 of *Synechococcus* sp. PCC 7002, a key residue for quinone-reductase site function and turnover of the cytochrome *bf* complex. *J. Biol. Chem. 280*, 10395–10402.
26. Zhang, H., Kurisu, G., Smith, J. L., and Cramer, W. A. (2003) A defined protein-detergent-lipid complex for crystallization of integral membrane proteins: The cytochrome b_6f complex of oxygenic photosynthesis. *Proc. Natl. Acad. Sci. U.S.A. 100*, 5160–5163.
27. Wenk, S. O., Boronowsky, U., Peterman, E. J. G., Jaeger, C., Van Amerongen, H., Dekker, J. P., and Roegner, M. (1998) Isolation and characterization of the cytochrome b_6f complex from the cyanobacterium *Synechocystis* PCC 6803, in *Photosynthesis: Mechanism and Effects* (Garab, G., Ed.) pp 1537–1540, Kluwer Academic Publisher, Dordrecht, The Netherlands.
28. Tsiotis, G., Lottspeich, F., and Michel, H. (1992) Isolation and characterization of cytochrome b_6f complex from *Synechocystis* PCC 6714, in *Research in Photosynthesis* (Murata, N., Ed.) pp 511–514, Kluwer, Dordrecht, The Netherlands.
29. Gray, K. A., Dutton, P. L., and Daldal, F. (1994) Requirement of histidine 217 for ubiquinone reductase activity (Qi site) in the cytochrome bc_1 complex. *Biochemistry 33*, 723–733.
30. Seely, G. R., and Connolly, J. S. (1986) Fluorescence of photosynthetic pigments in vitro, in *Light Emission by Plants and Bacteria* (Govindjee, Amesz, J., and Fork, D. C., Eds.) pp 99–133, Academic Press, New York.
31. Mataga, N., Chosrowjan, H., Taniguchi, S., Tanaka, F., Kido, N., and Kitamura, M. (2002) Femtosecond fluorescence dynamics of flavoproteins: Comparitive studies on flavodoxin, its site-directed mutants, and riboflavin binding protein regarding ultrafast electron transfer in protein nanospaces. *J. Phys. Chem. B 106*, 8917–8920.
32. van den Berg, P. A., van Hoek, A., Walentas, C. D., Perham, R. N., and Visser, A. J. (1998) Flavin fluorescence dynamics and photoinduced electron transfer in *Escherichia coli* glutathione reductase. *Biophys. J. 74*, 2046–2058.
33. Savikhin, S., Tao, N., Song, P. S., and Struve, W. S. (1993) Ultrafast pump-probe spectroscopy of the photoreceptor stentorins from the ciliate *Stentor coeruleus*. *J. Phys. Chem. 97*, 12379–12386.
34. Oba, T., and Tamiaki, H. (2002) Which side of the π-macrocycle plane of (bacterio)chlorophylls is favored for binding of the fifth ligand? *Photosynth. Res. 74*, 1–10.
35. Connolly, J. S., Samuel, E. B., and Janzen, A. F. (1982) Effects of solvent on the fluorescence properties of bacteriochlorophyll *a*. *Photochem. Photobiol. 36*, 565–574.
36. Zito, F., Finazzi, G., Joliot, P., and Wollman, F. A. (1998) Glu78, from the conserved PEWY sequence of subunit IV, has a key function in cytochrome b_6f turnover. *Biochemistry 37*, 10395–10403.
37. Pierre, Y., Breyton, C., Lemoine, Y., Robert, B., Vernotte, C., and Popot, J. L. (1997) On the presence and role of a molecule of chlorophyll *a* in the cytochrome b_6f complex. *J. Biol. Chem. 272*, 21901–21908.

BI702299B